

 Open access • Journal Article • DOI:10.1016/J.TRAC.2014.12.005

Multivariate calibration of NIR spectroscopic sensors for continuous glucose monitoring — [Source link](#)

Mohammad Goodarzi, Sandeep Sharma, Herman Ramon, Wouter Saeys

Institutions: Katholieke Universiteit Leuven

Published on: 01 Apr 2015 - Trends in Analytical Chemistry (Elsevier)

Related papers:

- [Non-invasive glucose monitoring technology in diabetes management: a review.](#)
- [Prospects and limitations of non-invasive blood glucose monitoring using near-infrared spectroscopy](#)
- [Recent advances in noninvasive glucose monitoring.](#)
- [In vivo noninvasive measurement of blood glucose by near-infrared diffuse-reflectance spectroscopy.](#)
- [Selection of the most informative near infrared spectroscopy wavebands for continuous glucose monitoring in human serum.](#)

Share this paper:    

View more about this paper here: <https://typeset.io/papers/multivariate-calibration-of-nir-spectroscopic-sensors-for-4hqjlt8xod>

Accepted Manuscript

Title: Multivariate calibration of NIR spectroscopic sensors for continuous glucose monitoring

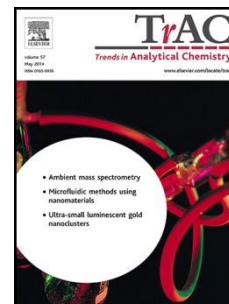
Author: Mohammad Goodarzi, Sandeep Sharma, Herman Ramon, Wouter Saeys

PII: S0165-9936(15)00026-6

DOI: <http://dx.doi.org/doi: 10.1016/j.trac.2014.12.005>

Reference: TRAC 14380

To appear in: *Trends in Analytical Chemistry*



Please cite this article as: Mohammad Goodarzi, Sandeep Sharma, Herman Ramon, Wouter Saeys, Multivariate calibration of NIR spectroscopic sensors for continuous glucose monitoring, *Trends in Analytical Chemistry* (2015), <http://dx.doi.org/doi: 10.1016/j.trac.2014.12.005>.

This is a PDF file of an unedited manuscript that has been accepted for publication. As a service to our customers we are providing this early version of the manuscript. The manuscript will undergo copyediting, typesetting, and review of the resulting proof before it is published in its final form. Please note that during the production process errors may be discovered which could affect the content, and all legal disclaimers that apply to the journal pertain.

Multivariate calibration of NIR spectroscopic sensors for continuous glucose monitoring

Mohammad Goodarzi *, Sandeep Sharma, Herman Ramon, Wouter Saeys

KU Leuven Department of Biosystems, MeBioS, Kasteelpark Arenberg 30, 3001 Leuven, Belgium

HIGHLIGHTS

- We review different measurement strategies for continuous glucose monitoring
- We elaborate the basic concepts of NIR spectroscopy for blood-glucose measurement
- We critically review chemometrics tools for glucose measurement from NIR spectra
- We set out research actions needed to advance glucose measurement from NIR spectra

ABSTRACT

Diabetes, a disorder in the control of blood-glucose levels, is one of the most serious metabolic diseases worldwide. Among the investigated technologies for continuous glucose monitoring (CGM), near-infrared spectroscopy (NIR) has received the most attention. There have been many attempts to develop NIR-based CGM systems with promising *in-vitro* results, but they lacked robustness for *in-vivo* use. We critically review the application of chemometrics for CGM and the research needed. Pre-processing and multivariate-calibration techniques, which allow exploiting expert knowledge on the potential interferences, are possible solutions. The combination and first overtone bands in the ranges 2050–2300 nm and 1500–1800 nm, respectively, are the most informative regions. We therefore recommended selecting the most informative variables and exploiting the available expert knowledge on known interferences in pre-processing or multivariate calibration to develop an NIR-based CGM sensor for *in-vivo* use.

Keywords:

Blood-glucose measurement
Chemometrics
Continuous glucose monitoring
Diabetes
In-vivo use
Multivariate calibration
NIR spectroscopy
Pre-processing strategy
Sensor
Variable selection

Abbreviations: (in standard style – alphabetical by abbreviation)

NIR	Near-infrared spectroscopy
CGM	Continuous glucose monitoring
WHO	World Health Organization
FDA	Food and Drug Administration
DCCT	Diabetes Care and Complications Trial
MIR	Mid-infrared
SNR	Signal-to-noise ratio
MLR	Multiple Linear Regression

PCA	Principal Component Analysis
PLSR	Partial Least Squares Regression
PCR	Principal Component Regression
ICA	Independent Component Analysis
ICR	Independent Component Regression
BSS	Blind source separation
DA	Direct calibration
CLS	Classical Least Squares
ACLS	Augmented Classical Least Squares
IDC	Improved direct calibration
SBC	Science-based calibration
NAS	Net analyte signal
RBFNN	Radial Basis Function Neural Network
SCMWPLS	Searching Combination Moving Window Partial Least Squares
GA	Genetic Algorithm
GS	Grid Search
LV	Latent variable
EMSC	Extended multiplicative signal correction
EISC	Extended inverse scatter correction
EPO	External parameter orthogonalization
GLSW	Generalized least squares weighting
OSC	Orthogonal signal correction
DF	Digital filtering
GSBDF	Gaussian-shaped bandpass digital filters
SEP	Standard error of prediction
RMSEC	Root mean squared error of calibration
RMSEP	Root mean squared error of prediction
RMSECV	Root mean squared error of cross validation
MSEP	Mean squared error of prediction
MSEC	Mean squared error of calibration
CV	Cross validation
MCCV	Monte Carlo cross validation
LOOCV	Leave-one-out cross validation
Lk-foldCV	Leave-more-out cross validation

* Corresponding author. Tel.: +32 16 37 71 19; Fax: +32 16 32 85 90.

E-mail addresses: mohammad.godarzi@gmail.com; Mohammad.goodarz@biw.kuleuven.be (M. Goodarzi)

1. Introduction

Diabetes, a disorder in the control of the blood-glucose level is considered to be one of the most serious metabolic diseases worldwide [1]. According to the World Health Organization (WHO) [2], about 60 million people or 10.3% of the male population and 9.6% of the female population in Europe suffer from diabetes. The situation is equally bad in the USA, where the Food and Drug Administration (FDA) reported that over 20 million people are affected [3]. The WHO estimates that around 3.4 million deaths are yearly caused by high blood-glucose levels [4]. Recently, it was predicted that the worldwide number of people with diabetes will increase from 246 million to 380 million by 2025 [5], while there still is no cure.

Persistent high blood-glucose levels can cause serious health complications, such as heart diseases, blindness, kidney failure, nerve damage and impaired wound healing, which often leads to lower-extremity amputations [6]. The Diabetes Care and Complications Trial (DCCT) demonstrated that tight glycaemic control delayed the onset of many of those complications and

that tight glycemic control was accomplished by frequent monitoring of blood glucose coupled with insulin therapy [7].

So far, the most successful way to control blood-glucose levels and delay onset of diabetic complications is through insulin therapy [8]. Proper use of insulin can prevent death from ketoacidosis in people with Type 1 or Type 2 diabetes and reduce complications due to chronic hyperglycemia in people with Type 2 diabetes [9]. The main purpose of insulin therapy is to prevent and to treat fasting and postprandial hyperglycemia [10], permit appropriate utilization of glucose and other nutrients by peripheral tissues [11] and suppress hepatic glucose production [12]. However, in insulin therapy, it is crucial to find a balance between two life-threatening extremes:

- when an insufficient dose of insulin is administered, the blood glucose cannot move from the blood into the cells, resulting in a high blood-glucose level (hyperglycemia) and burning of the fat and protein stores by the body, leading to the formation of ketone bodies (acetoacetate and β -hydroxybutyrate), which acidify the blood and cause metabolic acidosis; and,
- if too high a dose of insulin is administered, the blood-glucose level becomes too low (hypoglycemia) and may cause unconsciousness or, in severe cases, brain damage and coma [10].

2. Measurement strategies

Three different strategies have been proposed to measure glucose *in vivo*: invasive, minimal invasive and non-invasive (Fig. 1). Invasive techniques use optical or electrochemical glucometers, minimal invasive techniques can be categorized into transdermal approaches, glucose electrodes, microdialysis and open-flow microperfusion, and, finally, non-invasive techniques are subdivided into optical and non-optical techniques.

There are two invasive ways to measure blood glucose:

- in capillary blood, through the use of a finger prick; and,
- in venous blood, through the use of an indwelling vascular catheter [13].

The drawback of venous/arterial vascular blood sampling is that it bears a small risk of infections and that a low skin temperature (18°C) can cause underestimation of the blood-glucose concentration due to peripheral hypoperfusion, a condition where an organ or extremity does not receive sufficient blood [14,15].

Minimally invasive methods (e.g., subcutaneous implants) measure the glucose concentration in the interstitial fluid of the skin or in the subcutis, for example, by using an electrochemical sensor [16,17]. These techniques rely on the correlation between the concentration of glucose in blood and interstitial fluid (ISF) and allow for repeated blood-glucose monitoring [18,19] during days of operation. On the down side, glucose biosensors suffer from rapid performance deterioration after implantation due to surface fouling and coagulation caused by poor biocompatibility [20]. There is therefore a need to develop more reliable techniques, which allow accurate measurement inside human bodies.

Instead of using implantable sensors, it would be more desirable to monitor the glucose level continuously without pain and discomfort by not requiring piercing of the skin with a solid object to extract blood. A type of non-invasive CGM is based on non-optical techniques, which perform transdermal fluid extraction by compromising the epidermis with energy. Some techniques apply ultrasonic energy to the skin and measure the glucose concentration with a glucose-flux biosensor [21] or with electro-osmotic flow using reverse iontophoresis [22]. The

use of such devices for drug delivery or transdermal extraction of analytes of clinical interest is limited, due to their high cost and the risk of skin irritation [23,24].

Optical techniques, such as polarimetry [25], Raman spectroscopy [26], diffuse reflection spectroscopy [27,28], absorption spectroscopy [28, 29], thermal emission spectroscopy [30, 31], fluorescence spectroscopy [32] and photoacoustic (PA) spectroscopy [33,34], have been investigated to monitor levels of glucose in blood continuously in a non-invasive way. Several papers have reviewed different technologies in detail [35–37]. It was concluded by several authors that, although many attempts were made to measure glucose in biological tissues and some correlation exists between the measured optical signals and blood glucose, none could provide the proof that the measured signals correspond to the actual blood-glucose concentration [38]. Moreover, the development of a calibration model is challenging, because it must be robust enough to deal with light scattering caused by insoluble materials (e.g., fat and proteins) and to extract the often weak glucose signal from the complex biological matrix represented by the skin [36]. Tura et al. reviewed 14 optical technologies and 16 devices in detail according to quantitative criteria for glucose measurement [39].

From all these optical techniques, most attention has been given to near-infrared (NIR) spectroscopy, because of its ability to record spectra for solid and liquid samples with no prior manipulation, the availability of portable equipment and the cost of the equipment. More importantly, NIR radiation can penetrate up to several millimeters into human tissue, serum and interstitial fluid [40,41]. Despite NIR spectroscopy being considered the most promising technique for CGM and being investigated by many research groups [35,37,38], it has not yet led to a commercial sensor, mainly because many instruments, which gave promising results *in vitro*, turned out not to be robust enough to measure glucose *in vivo*.

2. Near-infrared spectroscopy

2.1. Basic concepts of near-infrared spectroscopy

The NIR region of the electromagnetic spectrum covers the wavelength range 750–2500 nm [42]. The absorption of NIR light in biofluids, such as blood or human serum, is mostly caused by the presence of C-H, O-H and N-H bonds, which can absorb photons with the right energy to excite overtone and combinations of fundamental molecular vibrations. The fundamental vibrations correspond to wavelengths in the mid-infrared (MIR). Glucose primarily absorbs NIR light in two distinct regions – the first overtone region at 1500–1800 nm and the combination-band region at 2050–2300 nm. NIR spectroscopic measurement of glucose in aqueous solutions is quite challenging due to the low concentration of glucose compared to that of water, resulting in a far smaller signal for glucose compared to that of water. Moreover, variations in blood pressure, body temperature and some environmental factors, such as humidity, temperature and pressure, have an impact on the NIR spectra acquired and complicate their interpretation.

2.2. Spectral basis for blood-glucose measurement

To estimate the pure component spectra, a high-concentration solution of glucose (120 mM) was prepared and its NIR spectra were measured. The molar absorptivity of glucose was calculated following the procedure described by Amerov et al. [43]. The molar absorptivities of water and glucose in the first overtone band are presented in Fig. 2 (a) and (b), respectively.

Similarly, the molar absorptivities of water and glucose in the combination band are presented in Fig. 2 (c) and (d), respectively. Two important observations can be made from Fig. 2. First, it can be seen that the molar absorptivity of glucose is higher in the combination band than in the first overtone band. This implies that the signal of glucose in the combination band is higher than in the first overtone band. Whether this also results in a higher signal-to-noise ratio (SNR) depends on the presence of chemical interferences and instrumental characteristics, such as light intensity and detector noise. Second, comparisons of Fig. 2 (a) with Fig. 2 (b) and Fig. 2 (c) with Fig. 2 (d) reveal that the molar absorptivity of glucose is higher than that of water by a factor of 4–6. However, in blood serum or interstitial fluid, the aqueous glucose spectrum will be dominated by the characteristic water absorption, because the total number of glucose molecules for a given volume is much smaller. For the physiological concentration of 3.9–7.2 mM glucose, the ratio varies from 14,000 to 8000.

Note that accurate calculations demand accounting for the impact of water displacement upon the dissolution of solute [43]. The phenomenon called water displacement is caused by the strong absorption of water throughout the NIR spectral region, leading to a significant change in absorbance spectra of dissolved solutes. In aqueous solutions, a specific molar volume of water is displaced by the solute molecules, resulting in fewer water molecules within the optical path of the spectroscopic measurement. Based on the relative magnitude of molar absorptivities of solute and water, negative absorbance values can be created, so the NIR spectra measured for aqueous solutions consist of both positive and negative absorbance regions.

3. Chemometrics

Due to the overlap between the absorption peaks of glucose and other molecules, there is no wavelength in the NIR spectrum that is only influenced by the glucose concentration, so the correlation of each individual wavelength variable with the glucose concentration is rather low and a univariate regression results in poor prediction of the glucose content. However, thanks to the broad absorption peaks in the first overtone and the combination bands, many wavelength variables are correlated to the glucose concentration. Moreover, the spectral signature of glucose is unique. These features make possible selective measurements of glucose by combining spectral information across a range of wavelengths.

Multivariate calibration (MC) plays an important role in extracting quantitative information from multivariate analytical data, such as NIR spectra. Geladi and Kowalski described it in very simple words: “Multivariate calibration means measuring a vector of properties (variables) for calibration standards of known content. This vector may be spectral intensities, current measurements or any relevant collection of data” [44]. The most straightforward way to build a MC is by using Multiple Linear Regression (MLR), where the dependent variable is modeled as a linear combination of the independent variables and the regression coefficients are estimated with the least squares criterion [45-47]. An MLR model could be shown as follows:

$$y = b_0 + b_1x_1 + b_2x_2 + \dots + b_mx_m \quad (1)$$

where y represents the estimated property (e.g., glucose concentrations), x_i the wavelength variables, and b_i the regression coefficients of the model.

However, this modeling technique cannot be used when the number of variables is larger than the number of samples, because there is then no unique solution to the least squares estimation of

the regression coefficients, a problem known as “exact multicollinearity” [48]. Even when the number of samples is larger than the number of variables, MLR may lead to poor prediction performance when the different variables are highly correlated. In this case, an individual variable can be approximately written as a linear combination of other variables, leading to unreliable estimates for the regression coefficients. This problem is known as “near-multicollinearity”. To overcome this problem, a biased regression can be used [49].

Many approaches have been developed to overcome the (near) multicollinearity problem. Among all these approaches, Partial Least Squares Regression (PLSR) is by far the most widely used technique in analytical chemistry [50–52].

Since the goal of MC is to understand the relationship between variables and observations, the degrees of freedom are a function of both the sample size and the number of independent variables. The degrees of freedom are equal to the number of samples minus the estimated number of parameters (e.g., slope). By increasing the sample size, the degrees of freedom also increase. By contrast, the degrees of freedom decrease by increasing the number of parameters. The number of degrees of freedom in a PCR model with k principal components (PCs) is $k+1$, due to the calculation of the mean spectrum for the mean-centering prior to the calculation of the PCs. So, to have sufficient power to estimate each of these degrees of freedom properly, it is recommended to use at least 6 times $k+1$ samples for building the model (ASTM E1655 - approved 2012 [53]). However, due to the definition of the latent variables (LVs) explaining maximal covariance between \mathbf{X} and \mathbf{y} , a PLS model can consume more than one degree of freedom per LV [54]. It is therefore recommended to build in some extra safety margin by using 10 times $k+1$ samples for building the model.

3.1. Partial Least Squares Regression

PLSR [55] is used for describing a given response (dependent variable) as a function of a few LVs, which are called PLS factors. The LVs are derived from the original variables as linear combinations, which maximally capture the covariance between the independent variables (data matrix of absorbance values) and the dependent variables (vector of analyte concentrations). The PLS model is built using the following equation:

$$\mathbf{X} = \mathbf{TP}^T + \mathbf{E} \quad (2)$$

$$\mathbf{y} = \mathbf{Tq} + \mathbf{e} = \mathbf{Xb} + \mathbf{e} \quad (3)$$

where \mathbf{X} is the data matrix, \mathbf{q} is the vector of regression coefficients associated with the PLS LVs (\mathbf{T}), and matrix \mathbf{E} and vector \mathbf{e} are the residuals representing the differences between the observed and predicted \mathbf{X} and the differences between the observed and predicted \mathbf{y} , respectively.

\mathbf{T} is the score matrix for both \mathbf{X} and \mathbf{y} , \mathbf{P} denotes the loading matrix. Scores are the projection of the samples onto the LVs. However, loadings are the projection of the LVs onto the original variables, which describe how the variables in the scores matrix \mathbf{T} relate to the original data. \mathbf{X} is the explanatory variables matrix and \mathbf{b} is the vector of regression coefficients. It can be calculated as:

$$\mathbf{b} = \mathbf{W}(\mathbf{P}^T\mathbf{W})^{-1}\mathbf{q} \quad (4)$$

where \mathbf{W} is a matrix of loadings maximizing the covariance criterion and \mathbf{P} is the result of the projection of \mathbf{X} onto the LVs.

3.1.1. Model complexity

A crucial aspect in building a biased regression model, like PCR and PLSR, is tuning the model complexity (i.e., the number of PCs for PCR or LVs for PLSR). As can be seen in Fig. 3, the bias for a built model decreases by increasing the model complexity (e.g., number of LVs), while the variance increases and *vice versa* [56,57]. The proper selection of PLS-model complexity (the best bias/variance trade-off) has always been questionable because, by selecting a few LVs, the model will produce bias in prediction, meaning that it leads to an under-fitted model. The opposite occurs by selecting too many LVs: the model built leads to overfitting with poor prediction ability due to spurious incorporated noise. Bias relates to the prediction-accuracy level of a model (e.g., how close the glucose-concentration values are to the predicted values). However, variance is the estimation error, which shows the level of uncertainty for the predicted values [58].

Special attention should therefore be paid to this step in model building. Selection of a proper number of PLS LVs has been a subject of interest to chemometricians developing new techniques [59–71] or comparing existing techniques [72–76]. To assess the quality of a calibration model, standard statistical measures are normally applied. The standard error of prediction (SEP) is a measure of the variability of the difference between the predicted and actual values (precision) for a set of samples and does not take the systematic deviation (bias) into account [77]. Therefore, calibration models should not be evaluated only based on the SEP. It is suggested to use other metrics, such as the root mean squared error of prediction (RMSEP), which measures the accuracy (difference between predicted and actual values) and thus combines both the SEP (variance) and the bias in one term. Typically, the model complexity is tuned based on the minimization of the prediction error in the validation. The most used techniques are based on cross validation (CV) [76], Monte Carlo CV (MCCV) [60–64], randomization [65,66] and bootstrapping [67-71].

Other metrics that include bias and variance information have been evaluated and discussed [54,79]. For example, Kalivas et al. [80] suggested using a variance indicator, such as the Euclidean norm (2-norm) of the regression coefficient vector $\|\mathbf{b}\|^2$ by plotting it against a bias metric. However, the RMSECV (root mean squared error of cross validation) is typically used to select the optimal number of LVs [78].

As mentioned above, CV techniques have been extensively used for tuning model complexity. One of the most popular CV techniques is Leave-One-Out CV (LOOCV). The idea behind an LOOCV method is to leave one sample out of a data set and use it for validation after building a model with remaining samples. This procedure is repeated in a way that each sample in the data set is used once as the validation data [81]. For larger sample numbers (> 20), there is a large risk that a sample very similar to the validation sample is also present in the calibration set. In this case, LOOCV will lead to the inclusion of unnecessary LVs, resulting in a better performance in CV, but a worse prediction ability of new samples (an over-fitted model). An Lk-foldCV would be a better choice for larger sample sets [82, 83]. It should be mentioned that LOOCV and k-fold CV or Lk-foldCV are conceptually the same, the only difference being that, in LOOCV, one sample is left out each time, while, in k-foldCV, several samples are left out.

It should be noted here that inverse modeling techniques, such as Principal Component Regression (PCR) and PLSR, are very sensitive to unspecific correlation between the spectral measurements and dependent variables present in the calibration data set. Such unspecific correlations can be caused by measurement artifacts that will not be persistent in the future. In order to safeguard against these, one should keep all related samples (e.g., measured on same day or for the same person) together in the calibration set or CV set [84].

3.1.2. Partial Least Squares Regression for glucose measurement from NIR spectra

Similar to other fields in analytical chemistry, PLSR has been the most frequently used inverse calibration method for predicting glucose concentration from spectroscopic signals. In a review paper, Arnold et al. [40] criticized the feasibility and the potential of non-invasive glucose monitoring for clinical blood-glucose measurements and bioreactor monitoring, because none of the existing patents published before 1996 provided a clear path or method for measuring glucose *in vivo* accurately. They concluded that, although some research groups had tried to measure glucose [85,86], none could prove that what was measured related to the glucose concentration, because subtle variations in spectra caused by, e.g., time or temperature might be correlated with glucose concentration. In these papers [85,86], the glucose level varied with time as spectra were collected, so the models built might have been based on this unspecific correlation.

Table 1 gives an overview of the data sets and the aims of different studies that have been devoted to glucose measurement from NIR spectra. As can be seen, the group led by Arnold has devoted special attention to this field. At first, they measured glucose in the physiological range (1–20 mM) in an aqueous matrix [87]. With a univariate calibration linking the absorbance at 2273 nm to the glucose concentrations, they obtained a prediction error of 0.3 mM on an external test set.

Several groups have investigated the effect of temperature variation on the accuracy of glucose measurement in an aqueous solution. In one paper [88], a PLS model was trained on spectra acquired at 37°C and tested on spectra measured at temperatures of 32–41°C at 1°C increments. By pre-processing the spectra with a digital Fourier filter method, the effect of temperature variation on glucose predictions could be minimized and an SEP of 0.14 mM (2.52 mg/dL) was obtained.

In another study, the NIR spectra of nine samples were measured at different temperatures (25°C, 30°C and 35°C) [89]. Three of those samples were used to build a PLS model and the remaining samples were used as the test set. When no preprocessing was applied before building the model, the first loadings vector obtained from the PLS model corresponded to the observed absorbance change caused by the temperature variation. This demonstrates that the PLS model incorporated the effect of temperature variation in the model. However, the data set used was rather small with a lack of sample to sample variation and no experimental design was used.

Other researchers have investigated the robustness of the glucose measurement from NIR spectra for other interferences, such as total protein concentration and glycated protein concentration [90,91]. To investigate the effect of the presence of protein on the glucose measurement, 97 spectra were collected from 14 glucose solutions over four days with glucose concentrations of 1.2–20.0 mM [92]. The protein concentration was 60.8 g/dl and constant for all solutions. The training and test set consisted of 67 and 34 spectra, respectively. The best PLS model using 14 LVs resulted in an SEP of 0.24 mM.

In another study, three different bovine plasma lots were used to prepare 69 glucose samples, 55 samples and 14 samples as training and test sets, respectively [93]. The best PLSR model resulted in an SEP of 0.37 mM.

To demonstrate the possibility of glucose measurement in samples with matrix variation, a series of binary mixture solutions of glucose and glutamine was prepared [94]. The concentration range of glucose and glutamine was 1.7–59.9 mM and 1.1–30.65 mM, respectively. A PLS model was built for each compound separately, resulting in SEPs of 0.32 mM and 0.75 mM for glucose and glutamine, respectively.

To increase the complexity of the matrix, mixtures of glucose, glutamine, glutamate, lactate and ammonia-nitrogen were prepared [95]. The NIR spectra of the corresponding 72 aqueous solutions were randomly split into a training set of 58 samples for PLSR model building and a test set of 14 samples for model validation. A PLSR model was built based on 12 LVs, which resulted in an SEP of 0.53 mM.

As the proteins and triglycerides present in serum-like solutions strongly overlap with the important absorption band of glucose around 2273 nm [96–98], it was investigated whether glucose can be measured in the presence of these molecules [99]. The PLS models resulted in SEPs of 0.5 mM and 0.2 mM in triacetin and bovine-serum albumin solutions, respectively.

As a continuous glucose sensor should be able to measure the glucose level in blood or serum, several studies have investigated the potential to measure glucose in human serum using NIR spectroscopy. A set of 242 undiluted human-serum samples was randomly split into 162, 40 and 40 samples as training, monitoring and test sets, respectively [100]. The monitoring set was used to optimize the calibration and the test set was used as a blind set to evaluate the prediction ability of the model built. The optimum PLS model using 14 LVs resulted in a 0.35 mM SEP. Another set of 50 serum samples, which had been measured before, were also used as a blind test set, resulting in an SEP of 2.91 mM. This indicates that the built model was not robust enough to handle the variation in different test sets, so the question of how to make a PLS model robust was highlighted by this study.

Afterwards, a comparison was made between the application of NIR and Raman in glucose monitoring [101]. Some 60 aqueous solutions consisting of glucose, lactate, and urea were measured with NIR and Raman spectroscopy. The acquired spectra were then used for PLS-model building. The data set was randomly split into 50 samples and 10 samples for training and test sets, respectively. The prediction ability of models built on NIR was better than for those built on the Raman data set. The SEP values obtained with PLS on the NIR data were 0.24 mM, 0.11 mM and 0.14 mM for glucose, lactate and urea, respectively, while they were 0.40 mM, 0.42 mM and 0.36 mM for the PLS models built on the Raman spectra.

It should be noted that some studies were based on simulated data [102–104]. However, the results obtained for the models built in these studies were limited to those simulated data so we do not discuss them in this review.

3.2. Alternative calibration methods for glucose measurement from NIR spectra

In the previous section, we concluded that, although PLSR is able to capture both specific and unspecific covariance between the acquired spectral signals and the glucose content, it may result in MC models that are not robust enough for practical use, so other MC strategies were proposed.

3.2.1. Independent Component Analysis

Independent Component Analysis (ICA), also known as Blind Source Separation (BSS) [105], aims to find the independent sources contributing to a mixed signal (e.g., an NIR spectrum). This is done by assuming that the data variables are linear mixtures of some unknown LVs. The LVs are assumed to be non-Gaussian and mutually independent, and are called the independent components of the observed data [106]. Linear ICA can be presented as [Equation (5)]:

$$\mathbf{X} = \mathbf{AS} + \mathbf{E} \quad (5)$$

where \mathbf{X} is an $m \times n$ matrix of m measured mixture spectra (absorbance values in the case of the Beer-Lambert law) for the p variables (e.g., wavelengths) and the n samples, \mathbf{A} is an $m \times k$ mixing matrix, \mathbf{S} is a $k \times n$ matrix of k independent components, and \mathbf{E} is the matrix of residual spectra.

This technique has also been evaluated for glucose measurement [107]. Some 90 NIR spectra were collected for 30 mixtures of a matrix prepared by dissolving glucose, urea and triacetin in a phosphate-buffer solution. The model was trained on 20 samples and tested on 10 different samples. The data matrix was decomposed into Scores, Loadings and Eigenvalues using PCA. The Scores matrix was then used as an input for ICA. The estimated mixing and independent components were obtained by ICA, and relative concentration levels of each component (A) in the mixtures were used to build an MLR model. Independent Component Regression (ICR) was built by using the selected number of scores from the PCA model as the input to ICA algorithm. The numbers of factors for ICR, PCA-ICR and PLS were 16, 18 and 13, respectively. PCA-ICR outperformed PLS and ICR with an SEP of 1.34 mM compared to 1.97 mM and 1.61 mM for PLS and ICR, respectively.

3.2.2. Direct calibration methods

The added value of expert knowledge in improving the robustness of MC models for glucose prediction was demonstrated [108]. Although Classical Least Squares (CLS) has been reported to be a useful technique for extracting qualitative information [109], it is rather limited when, e.g., the concentration of one or more compounds in a mixture is unknown. The CLS model is mathematically written as [Equation (6)]:

$$\mathbf{X} = \mathbf{CK} + \mathbf{E} \quad (6)$$

where \mathbf{X} is the $m \times n$ matrix of m measured mixture spectra (as described above), \mathbf{C} is the $m \times p$ matrix of concentration values for the p components, \mathbf{K} is the $p \times n$ matrix of the pure component signals (e.g., spectra) at unit concentration, and \mathbf{E} is the matrix of residual spectra.

To overcome this limitation of CLS, it has been proposed to estimate the contributions of the unknown components and augment the CLS equation. This method is known as augmented Classical Least Squares (ACLS) [110], which is done by augmenting the concentration matrix during the CLS calibration procedure [111] or augmenting the pure component spectral signal matrix [112,113]. The unknown components to be added in the augmentation can be estimated from the calibration set at hand [112,113], from a noise matrix (PACLS and IDC) [111], or directly measured for known interferences for which the concentrations are unknown [114]. After augmentation of the pure component matrix, the spectral measurements are corrected from the interferences and then projected onto the pure component spectrum in order to obtain the coefficient vector, which can then be used further to predict an unknown sample [115].

Science-based calibration (SBC) is another direct calibration method inspired by a modular method in signal processing, known as Wiener filtering. It aims to isolate the analyte signal from the spectral noise without using costly reference values. The regression-coefficient vector is calculated by weighting the pure component spectrum of the analyte of interest with an estimate for the noise-covariance matrix [116,117]. However, the net analyte signal (NAS) is the part of the pure component spectrum that is orthogonal to the interferents. Projecting \mathbf{X} to \mathbf{Y} in an attempt to remove the spectral information in \mathbf{X} , which is orthogonal to \mathbf{y} , is a method known as net analyte preprocessing (NAP).

The prediction performance and robustness of NAP, IDC, SBC and ACLS using different amounts of expert knowledge have been evaluated and benchmarked against conventional PLS [108]. It was reported that the inclusion of expert knowledge in these alternative calibration techniques was found to reduce the dramatic effects of a change in the interferent structure on the prediction performance, even when the interferent structures in the test and training sets were different from each other. The ACLS model led to the best result when the pure component spectra of the analyte of interest and the interferents were incorporated. Hereby, the RMSEP was reduced by a factor 3 compared to conventional PLS when the test set had a different interferent structure than the calibration set for a similar range of glucose concentrations.

3.2.3. Non-linear regression methods

Light scattering and molecular interactions can cause (non-linear) deviations from the linear additive relation between the analyte concentrations and the acquired absorbance signals. In such cases, methods relying on the Beer-Lambert law may no longer be appropriate and non-linear calibration methods may be needed. The Radial Basis Function Neural Network (RBFNN) is a standard feed-forward neural network including three layers: an input layer, a Gaussian (RBF) function hidden layer and an output layer. The input layer consists of, e.g., NIR spectra, while the output layer contains the corresponding concentration values. The goal of an RBF network is to generate proper weights and biases connected between the input and the hidden layers, and between the hidden layers and the output target. This results in an output that is a linear combination of RBFs of the inputs and hidden layers [118]. More details are available [119,120].

Fischbacher et al. compared the performance of RBFNN with PLSR in predicting the blood-glucose level from 150 diffuse reflectance spectra in the 850–1300-nm range obtained through the fingers of three Type-1 people with diabetes [121]. The number of hidden neurons, which affects the performance of the RBFNN, was optimized by LOOCV. RBFNN outperformed PLS regression with RMSEP values of 1.4 mM and 1.9 mM, respectively. Although the non-linear technique led to a considerable improvement in prediction, it was a rather complex modeling technique and more difficult to tune. Note that the 1.4 mM and 1.9 mM values probably represent measurements based on changes in refractive index or spurious correlations; however, it is unlikely that the information in these calibration models originated from the spectrum of glucose due to the lack of glucose information in this spectral range.

3.3. Variable selection

Normally, data sets acquired with analytical instruments, such as NIR spectroscopy, contain many irrelevant features. By removing those irrelevant features, the prediction performance and robustness of the calibration models can be improved, so reducing the dimension of a multivariate data set is one of the most important steps in data handling. Variable-selection and

reduction techniques are used to simplify the interpretation of models with few variables, to improve the prediction performance, and to decrease the risk of overfitting and overtraining [122].

In order to investigate the most informative part of the NIR spectra for glucose measurement, a variable-selection technique [e.g., Genetic Algorithm (GA)] was used or the spectra were manually split into several wavelength ranges and different models were built. In the latter case, the region that led to a better performance model was chosen to be the most informative region. Table 1 summarizes the aims of different reported studies, which mostly followed the latter strategy, e.g. [92], seven different spectral regions were examined based on three different glucose bands around 2128 nm, 2273 nm and 2325 nm. It was found that the most informative wavelength range was 2174–2326 nm, while the prediction ability of the PLS model decreases using the full spectrum. The same conclusions were drawn from glucose measurements under changing temperatures [99] and in undiluted plasma matrices [92]. The C-H combination band at 2273 nm has proved to be the most useful band for building glucose-calibration models [44,88,92,93,123].

Searching Combination Moving Window Partial Least Squares (SCMWPLS) is a wavelength-selection technique that searches the most relevant set based on a combination of informative regions or an optimized individual informative region. This strategy is quite simple and very similar to a forward selection started by setting a window size at the i^{th} spectral channel and ending at the $(i^{\text{th}} + \text{window size} - 1)$. SCMWPLS has been evaluated to quantify glucose *in vitro* (bovine-serum samples) and *in vivo* (human-skin samples) [124]. The 1280–1849 nm range was selected for the 45 bovine-serum samples and the 1212–1889 nm range was selected for the 48 human-skin samples. The optimized informative region for the *in-vitro* data set was found to be the combination of four informative regions of 1373–1429 nm, 1495–1545 nm, 1565–1696 nm and 1790–1805 nm, while, for the *in-vivo* data set, only one optimized informative region of 1616–1733 nm was recognized. The best model for the *in-vitro* data set led to an RMSECV of 1.40 mM and a correlation coefficient of 0.99 for eight PLS factors, while the best model for the *in-vivo* data set used the 1616–1733 nm region and resulted in a correlation coefficient of 0.92, an RMSECV of 0.95 mM and four LVs. It should be noted that these are CV results of segments, which might be overoptimistic, as the model complexity was selected to minimize the CV error, so these results should still be validated on an independent test set.

GAs are a well-known technique inspired by the concepts underlying evolution [125] to optimize the position and the width of the bandpass digital filter, wavelength and LV selections [126]. Shaffer et al. applied this technique to two sets of data:

- the first was glucose in a phosphate-buffer matrix, including bovine serum albumin and triacetin (GTB); and,
- the second was glucose in a human-serum matrix (serum).

The prediction ability of models built based on three different fitness functions used in a GA process was investigated. The fitness functions used were based on the combination of Mean Squared Error of Calibration (MSEC) or Mean Squared Error of Prediction (MSEP) with the number of LVs, or a combination of both MSEC and MSEP with the number of LVs together. GA was compared to Grid Search (GS). The SEP for the GS-coupled PLS model using the GTB data set (spectral range 2242–2321 nm) and serum data set (spectral range 2062–2353 nm) were 0.91 mM and 1.20 mM, respectively. However, the SEP for the GA-coupled PLS model using the GTB data set (spectral range 2174–2328 nm) and serum data set (spectral range 2085–2325 nm) were 0.66 mM and 1.18 mM, respectively.

In another study, the same authors used three data sets. The first one was glucose free and the two others (GTB and serum data sets) were taken from on paper [127]. The SEPs of the PLS models, built on the 2000–2500 nm range (519 spectral points) for GTB and serum data sets, were 8.60 mM and 8.96 mM, respectively. Afterwards, they used GA to select the best region from 2000–2500 nm for both data sets. It was found that GA selected 153 and 230 spectral points for GTB and serum data, which were in the range 2081–2381 nm. The SEPs for GA-PLS for GTB and serum data sets were 0.64 mM and 1.13 mM, respectively. They concluded that the ranges of 2128–2326 nm and 2000–2083 nm included noise. In order to prove this, they built a PLS model for both data sets using the 2081–2381 nm wavelength range (312 spectral points). The SEP of PLS models for GTB and serum were 0.59 mM and 1.39 mM, respectively. Based on their observation, it was concluded that the glucose bands were located in the 2083–2381-nm range, while the ranges of 2128–2326 nm and 2000–2083 nm included noise.

However, a GS was also applied on the same data set and resulted in selection of spectral ranges of 2119–2328 nm and 2061–2353 nm for data sets of GTB and serum, respectively. The SEP for GS-PLS for GTB and serum data sets were 0.66 mM and 1.36 mM, respectively. It was therefore concluded that GA was superior to not only GS, but also the built PLS models without performing any variable selection [127]. In another study [128], the same data set [126,127] was used and the same conclusion was drawn.

Several research groups [129–132] investigated the question as to whether the first overtone band (1500–1800nm) or the combination band (2050–2300 nm) is the most informative. A comparison was made between PLS models built using the first overtone band and the combination band to measure glucose, lactate, urea, ascorbate, triacetin, and alanine in aqueous solutions [129]. Sample thicknesses, which affected the spectral quality, were 7.5 mm and 1.5 mm for the first overtone and combination bands, respectively. Some 80 samples were split into training, monitoring and external test sets, consisting of 50, 15 and 15 samples, respectively. The PLS models for glucose resulted in SEPs of 1.12 mM and 0.45 mM for the first overtone and combination-band spectra, respectively.

In another study, the first overtone and combination bands were compared for analyte measurements in aqueous solutions consisting of glucose, lactate, urea, ascorbate, triacetin and alanine [130–132]. In one paper [130], the best region was mentioned to be 2036–2324 nm, while it was reported [131] that a combination of the regions (1473–1831 nm and 2111–2374 nm) provided the best glucose-prediction accuracy.

Furthermore, a grid search was used to find the optimal spectral range [132]. PLS models were built over the combination, first-overtone and short-wavelength spectral regions using 80 different samples prepared from a single whole-blood matrix [132]. The SEP values obtained were 0.96 mM, 1.20 mM and 2.53 mM for combination band, first-overtone band and short-wavelength regions, respectively. The authors tried 5100 combinations of spectral ranges, using model complexities of 1–15 LVs. The best spectral range within the combination band (2000–2500 nm) was 2062–2381 nm. This spectral range consists of several known glucose-absorption features, centered at 2123 nm, 2272 nm and 2325 nm, which were used by the PLS models [87]. The best spectral range in the first-overtone and short-wavelength spectral region (1111–1852 nm) was found through the grid search to be 1550–1754 nm. This selected region is situated in the first-overtone band and corresponds to several known glucose-absorption features centered at 1613 nm, 1689 nm and 1731 nm [133]. The authors concluded that the exclusion of the short-wavelength range from the optimized range is because this region is dominated by scattering. Moreover, this region lacks glucose-specific absorption features.

3.4. Preprocessing

Irrelevant variation in the acquired spectra due to measurement noise and background interferences can obscure the information on chemical variations in the analyte and increase the complexity of an MC model [57,134–136]. Different preprocessing techniques have therefore been proposed to remove the irrelevant variations and the background interferences from NIR spectra. A preprocessing technique does not necessarily improve the prediction ability, but can result in more parsimonious models that are expected to be more robust, thanks to the removal of unwanted variation (e.g., instrumental artifacts).

Preprocessing techniques are normally used to adjust the variability of a measured variable (e.g., normalization or scaling) or to deal with typical artifacts for a given type of data (e.g., baseline correction). As discussed in a critical review on the selection of preprocessing techniques before data analysis [135], a complete pre-processing strategy for a given NIR data consists of the following steps:

- (1) baseline correction;
- (2) scatter correction;
- (3) noise removal; and
- (4) scaling.

In this review, we categorize the pre-processing methods into four classes (with details in the Supplementary material):

- (1) spectroscopic transformations;
- (2) scatter and baseline correction;
- (3) interference removal; and,
- (4) variable weighting.

The use of prior information in preprocessing techniques (EMSC, EISC, EPO and GLSW) was demonstrated to improve the robustness of the PLS for modeling glucose [137]. This study was carried out on two data sets:

- NIR spectra of aqueous solutions containing glucose, D-lactate and urea; and,
- NIR spectra of powder mixtures containing glucose, lactate and casein.

In the aqueous solution data set, a representative training set was provided for the calibration. In this case, it was demonstrated that the use of prior information could result into more accurate models, as discussed in many other cases [139,140].

In the powder-mixture data set, the training and test sets were designed to have different interferent structures. As expected, the conventional PLS model was unable to cope with the change in interferent structure in the test set. In this case, the use of prior information in the model calibration step or in the preprocessing step resulted in a considerable reduction of the prediction error. It was concluded from this study that some preprocessing techniques, which use expert knowledge, successfully reduce the sensitivity of the resulting models to changes in the interferent structure. Among the preprocessing techniques using expert information, Spectral Interference Subtraction (SIS) was found to be an effective technique for both data sets used. Moreover, EPO, GLSW and EMSC were effective for only one data set.

The key advantage of using these techniques is that they relax the requirement for a “representative” calibration set, so they open up perspectives for more efficient, economical MC model building. The approach adopted by the authors is especially interesting for glucose

measurements in biological fluids, such as human serum or interstitial fluid, where it is nearly impossible to obtain a “representative” calibration set for training the multivariate model.

Of all orthogonal projection techniques, most attention has been given to the orthogonal signal correction (OSC) method, which was developed to remove systematic variation in the spectra that are not correlated to the response values. There are many versions of OSC techniques, which have been discussed in detail and compared [137,138].

Du et al. [141] tried to use OSC for removing interfering signals in the first overtone band of glucose in blood at 1212–1889 nm. Although they aimed to develop a novel technique, their technique is just original OSC using a limited spectral region to estimate the scores and the loading weights of the orthogonal components to pretreat the spectra in the other regions. In the range 1600–1730 nm, it was found that ROSC-PLS led to an RMSECV of 0.88 mM, while the RMSECV values for PLS and OSC-PLS RMSECV were 0.95 mM and 0.95 mM, respectively.

Digital filtering was also used as a preprocessing step before PLS modeling to remove spectral features not associated with glucose [92,93]. For example, Gaussian-shaped bandpass digital filters (GSBDF) were implemented using the Fourier filtering technique to reduce both high-frequency noise and baseline variations [92]. The measurements of glucose at clinically relevant concentrations in a buffered-protein matrix [93] and the measurement in three unique undiluted plasma matrices were investigated for a PLS model and a digital filtering-PLS model. The authors optimized the number of LVs using a training set by varying the number of LVs from 1 to 20 and choosing the one with the lowest SEP. They reported that, in spite of a strong overlap between the absorption peaks of glucose and those from the matrix components, such as triacetin and protein, a PLS model could be built and predict accurately. By comparing the results obtained for PLS and DFF-PLS, the authors reported significant improvements of 53% and 70% in SEP for calibration and test sets, respectively.

Using the NAS technique [101,108,129,132] demonstrated the selectivity of the combination-band region for quantifying solutes in aqueous solutions. The quality of the spectral signal of the solutes and their distinction were determined using an NAS vector. It was found that the models based on the combination band resulted in a three-fold lower SEP than those for the first-overtone band. This was found by NAS, which is the portion of the solute spectrum orthogonal to all other sources of spectral variance in the data. The larger the NAS indicates, the greater the distinction is [129,132]. Although NAS led to a better result, the model performance was rather similar to that of conventional PLS. It was shown that the SEP obtained for glucose was 0.24 mM using both conventional PLS and NAS [101]. Furthermore, two approaches were used to estimate the noise matrix for NAS [108]. The first was by orthogonal projection of calibration spectra on the glucose concentration, and the second was by subtracting the contribution of glucose from measured spectra. The RMSEP for conventional PLS was 1.08 mM while the RMSEPs for NAS were 0.99 mM and 0.88 mM, when the first and second approaches were used to define the noise matrix, respectively, indicating that the second approach led to a better prediction performance than that of conventional PLS and classical NAS [108].

5. Conclusion, predictions and future directions

Although there has been a lot of research done on different technologies and devices for continuous glucose monitoring, so far, none has produced a commercially-available, clinically-reliable device. Great attention has been given to NIR spectroscopy as a promising technique for continuous glucose monitoring. Due to the broad, overlapping absorption peaks in the NIR, MC

methods are needed to extract the information on the glucose content from the spectra acquired. PLSR was by far the most used technique. As these statistical techniques rely on the calibration samples to estimate the relation between NIR spectra and the glucose concentration, they are very sensitive to the presence of outliers and unspecific correlations. Proper experimental design and model validation are essential to obtain robust calibration models. There have been many attempts to develop a CGM system based on NIR spectroscopy, for which promising *in-vitro* results have been reported, but it turned out not to be robust enough for *in-vivo* use. For many other studies, proper validation has not been reported.

For many properly validated calibration models, the reported SEP values are above 3 mM, which, according to the Clarke error grid, is too high to be acceptable for home glucose meters. More importantly, it was found that PLS fails when there is unexpected variation. In order to overcome this problem, alternative calibration methods have been proposed and shown promising results. From the wavelength regions considered in the NIR range, the combination-band region of 2050–2300 nm has been reported to be the most informative, followed by the first-overtone region ranging of 1500–1800 nm.

In addition, different preprocessing techniques have been applied to build a more robust PLS model for glucose measurements. Of all the different preprocessing techniques, it was found that those techniques that use expert knowledge to produce PLS calibration models are more robust against changes in the interferent levels not covered in the calibration set.

In conclusion, selection of the most informative variables, proper spectral preprocessing and incorporation of expert knowledge in the MC should be considered when building a calibration model for an NIR-based CGM sensor that is robust enough for *in-vivo* use.

Acknowledgment

The authors gratefully acknowledge I.W.T. Flanders for the financial support through the Chameleon project (IWT 100021) and GlucoSens project (SB-090053).

References

- [1] J.P. Auses, S.L. Cook, J.T. Maloy, Chemiluminescent enzyme method for glucose, *Analytical Chemistry*, 47 (1975) 244-249.
- [2] <http://www.euro.who.int/en/what-we-do/health-topics/noncommunicable-diseases/diabetes/news/news/2011/11/diabetes-epidemic-in-europe> (accessed 29 January 2014)
- [3] <http://www.fda.gov/ForConsumers/ByAudience/ForWomen/WomensHealthTopics/ucm117969.htm> (accessed 29 January 2014)
- [4] WHO, "Diabetes," <http://www.who.int/mediacentre/factsheets/fs312/en/>.
- [5] R. Sicree, *Diabetes Atlas*, Third edition, International Diabetes Federation, Brussels, 2008.
- [6] T. Jeffery, M.D. Wieman, Principles of management: the diabetic foot, *The American Journal of Surgery*, 190 (2005) 295–299.
- [7] S. Auxter, Disease Management Models of Diabetes Take Root. *Clinical Chemistry News* November, (1996) 5 – 16
- [8] J.W. Yoon, H.S. Jun, Recent advances in insulin gene therapy for Type 1 diabetes, *Trends in Molecular Medicine*, 8 (2002) 62-68.

- [9] R.A. Rizza, Pathogenesis of Fasting and Postprandial Hyperglycemia in Type 2 Diabetes: Implications for Therapy, *Diabetes*, 59 (2010) 2697–2707.
- [10] S. Heller, Hypoglycaemia in diabetes, *Medicine*, 38 (2010) 671-675.
- [11] H. Elrick, R. Purnell, the response of kidney, liver, and peripheral tissues to tolbutamide and insulin, *Ann N Y Acad Sci*, 71 (1957) 38-45.
- [12] A.D. Cherrington, D. Edgerton, D.K. Sindelar, The direct and indirect effects of insulin on hepatic glucose production in vivo, *Diabetologia*, 41 (1998) 987-996.
- [13] A.M. Kelly, The case for venous rather than arterial blood gases in diabetic ketoacidosis, *Emerg Med Australas*, 18 (2006) 64-67.
- [14] A. Haupt, B. Berg, P. Paschen, M. Dreyer, H.U. Haring, J. Smedegaard, S. Matthaei, The effects of skin temperature and testing site on blood glucose measurements taken by a modern blood glucose monitoring device, *Diabetes Technol Ther*, 7(2005) 597–601.
- [15] L. Heinemann, Finger Pricking and Pain: A Never Ending Story, *Journal of Diabetes Science and Technology*, 2 (2008) 919-921.
- [16] B.J. Privett, J.H. Shin, M.H. Schoenfish, *Electrochemical Sensors*, *Anal Chem*, 82 (2010) 4723-4741.
- [17] D.B. Keenan, J.J. Mastrototaro, G. Voskanyan, G.M. Steil, Delays in Minimally Invasive Continuous Glucose Monitoring Devices: A Review of Current Technology, *Journal of Diabetes Science and Technology*, 3 (2009) 1207-1214.
- [18] S. Darzi, Y. Munz, The Impact of Minimally Invasive Surgical Techniques, *Annual Review of Medicine*, 55 (2004) 223-237.
- [19] S.N. Thennadil, J.L. Rennert, B.J. Wenzel, K.H. Hazen, T.L. Ruchti, M.B. Block, Comparison of glucose concentration in interstitial fluid, and capillary and venous blood during rapid changes in blood glucose levels, *Diabetes Technol Ther*, 3 (2001) 357-365.
- [20] T. Koschinsky, L. Heinemann, Sensors for glucose monitoring: technical and clinical aspects, *Diabetes Metab Res Rev*, 17 (2001) 113-123
- [21] H. Chuang, E. Taylor, T.W. Davison, Clinical evaluation of a continuous minimally invasive glucose flux sensor placed over ultrasonically permeated skin, *Diabetes Technol Ther*, 6 (2004) 21-30.
- [22] J.A. Tamada, S. Garg, L. Jovanovic, K.R. Pitzer, S. Fermi, R.O. Potts, Noninvasive glucose monitoring: comprehensive clinical results, Cygnus Research Team. *JAMA*, 282 (1999) 1839-1844.
- [23] H.P. Chase, R. Beck, W. Tamborlane, B. Buckingham, N. Mauras, E. Tsalikian, T. Wysocki, S. Weinzimer, C. Kollman, K. Ruedy, D.A. Xing, Randomized multicenter trial comparing the GlucoWatch Biographer with standard glucose monitoring in children with Type 1 diabetes, *Diabetes Care*, 28 (2005) 1101-1106.
- [24] J.A. Tamada, T.L. Davis, A.D. Leptien, J. Lee, B. Wang, M. Lopatin, C. Wei, D. Wilson, K. Comyns, R.C. Eastman, The effect of preapplication of corticosteroids on skin irritation and performance of the GlucoWatch G2 Biographer, *Diabetes Technol Ther*, 6 (2004) 357-367.
- [25] B.H. Malik, Real-time, closed-loop dual-wavelength optical polarimetry for glucose monitoring, *J. Biomed.Opt*, 15 (2010) 017002.
- [26] A.M.K. Enejder, T.G. Seccina, J. Oh, M. Hunter, W. Shih, S. Sasic, G.L. Horowitz, M.S. Feld, Raman spectroscopy for noninvasive glucose measurements, *J. Biomed. Opt*, 10 (2005) 031114.
- [27] K. Maruo, M. Tsurugi, M. Tamura, Y. Ozaki, In vivo noninvasive measurement of blood glucose by nearinfrared diffuse-reflectance spectroscopy, *Appl. Spectrosc*, 57 (2003) 1236–1244.

- [28] C. Vrancic, A. Fomichova, N. Gretz, C. Herrmann, S. Neudecker, A. Pucci, W. Petrich, Continuous glucose monitoring by means of mid-infrared transmission laser spectroscopy in vitro, *Analyst*, 136 (2011) 1192–1198.
- [29] I. Gabriely, R. Wozniak, M. Mevorach, J. Kaplan, Y. Aharon, H. Shamon, Transcutaneous glucose measurement using near-infrared spectroscopy during hypoglycemia, *Diabetes Care*, 22 (1999) 2026–2032.
- [30] C.D. Malchoff, K. Shoukri, J.I. Landau, J.M. Buchert, A novel noninvasive blood glucose monitor, *Diabetes Care*, 25 (2002) 2268–2275.
- [31] X. Guo, A. Mandelis, A. Matvienko, K. Sivagurunathan, B. Zinman, Wavelength-modulated differential laser photothermal radiometry for blood glucose measurements, *J. Phys. Conf. Ser.*, 214 (2010) 012025.
- [32] R. Ballerstadt, C. Evans, A. Gowda, R. McNichols, In vivo performance evaluation of a transdermal nearinfrared fluorescence resonance energy transfer affinity sensor for continuous glucose monitoring, *Diabetes Technol. Ther.*, 8 (2006) 296–311.
- [33] J. Kottmann, J.M. Rey, M.W. Sigrist, New photoacoustic cell design for studying aqueous solutions and gels, *Rev. Sci. Instrum.*, 82 (2011) 084903.
- [34] H.A. MacKenzie, H. Ashton, S. Spiers, Y. Shen, Advances in photoacoustic noninvasive glucose testing, *Clin. Chem.*, 45 (1999) 1587-1595.
- [35] O.S. Khalil, Non-invasive glucose measurement technologies: an update from 1999 to the dawn of the new millennium, *Diabetes Technol. Ther.*, 6 (2004) 660–697.
- [36] A. Sieg, R.H. Guy, M.B. Delgado-Charro, Noninvasive and minimally invasive methods for transdermal glucose monitoring, *Diabetes Technol. Ther.*, 7 (2005) 174-197.
- [37] O.S. Khalil, Spectroscopic and clinical aspects of noninvasive glucose measurements, *Clin Chem.*, 45 (1999) 165-177.
- [38] M.A. Arnold, Non-invasive glucose monitoring, *Curr Opin Biotechnol.*, 7 (1996) 46-55.
- [39] A. Tura, A. Maran, G. Pacini, Non-invasive glucose monitoring: Assessment of technologies and devices according to quantitative criteria, *Diabetes Research and Clinical Practice*, 77 (2007) 16-40.
- [40] M. Blanco, I. Villarroya, NIR spectroscopy: a rapid-response analytical Tool, *Trends in analytical chemistry*, 21 (2002) 240- 250
- [41] G. Hong, J.C. Lee, J.T. Robinson, U. Raaz, L. Xie, N.F. Huang, J.P. Cooke, H. Dai, Multifunctional in vivo vascular imaging using near-infrared II fluorescence, *Nature Medicine*, 18 (2012) 1841–1846.
- [42] S.F. Malin, T.L. Ruchti, T.B. Blank, S.N. Thennadil, S.L. Monfre, Noninvasive prediction of glucose by near-infrared diffuse reflectance spectroscopy, *Clin. Chem.*, 45 (1999) 1651-1658.
- [43] A.K. Amerov, J.Chen, M.A. Arnold, Molar absorptivities of glucose and other biological molecules in aqueous solutions over the first overtone and combination regions of the near-infrared spectrum, *Appl. Spectrosc.*, 58 (2004) 1195-1204.
- [44] P. Geladi, B.R. Kowalski, an example of 2-block predictive partial least-squares regression with simulated data, *Analytica Chimica Acta*, 185 (1986) 19-32.
- [45] R. Bro, Multivariate calibration What is in chemometrics for the analytical chemist?, *Analytica Chimica Acta*, 500 (2003) 185–194.
- [46] T. Næs, T. Isaksson, T. Fearn, T. Davies, *A User-Friendly Guide to Multivariate Calibration and Classification*. NIR Publications: Chichester, UK. 2002.
- [47] R.G. Brereton, *Chemometrics: Data Analysis for the Laboratory and Chemical Plant*. J. Wiley and Sons: New York, NY. 2003

- [48] M. Goodarzi, S. Funar-Timofei, Y. Vander Heyden, Towards better understanding of feature-selection or reduction techniques for Quantitative Structure–Activity Relationship models, *Trends in Analytical Chemistry*, 42 (2013) 49-63.
- [49] P. Geladi, B.R. Kowalski, Partial Least-Squares Regression: A tutorial, *Analytica Chimica Acta*, 186 (1986) 1-17
- [50] S. Wold, H. Martens, H. Wold, The multivariate calibration problem in chemistry solved by the PLS method, *Lecture Notes in Mathematics*, 973 (1983) 286-293.
- [51] P.D. Wentzell, L.V. Montoto, Comparison of principal components regression and partial least squares regression through generic simulations of complex mixtures, *Chemometrics and Intelligent Laboratory Systems*, 65 (2003) 257– 279
- [52] J.H. Kalivas, Multivariate Calibration, an Overview, *Analytical Letters*, 38 (2005) 2259–2279
- [53] ASTM Standard E1655, 2012: Standard practices for infrared multivariate quantitative analysis. West Conshohocken, PA: ASTM International; 2012, doi:10.1520/E1655-05R12, <www.astm.org>.
- [54] N. Krämer, M. Sugiyama, The Degrees of Freedom of Partial Least Squares Regression. *Journal of the American Statistical Association*, 106 (2011) 697-705.
- [55] S. Wold, M. Sjöström, L. Eriksson, PLS-regression: a basic tool of chemometrics, *Chemometrics and Intelligent Laboratory Systems*, 58 (2001) 109-130.
- [56] N.M. Faber, A closer look at the bias-variance trade-off in multivariate calibration, *J. Chemometrics*, 13 (1999) 185–192.
- [57] O.E. De Noord, The influence of data preprocessing on the robustness and parsimony of multivariate calibration models, *Chemometrics and Intelligent Laboratory Systems*, 23 (1994) 65-70
- [58] T. Naes, H. Martens, Principal component regression in NIR analysis: Viewpoints, background details and selection of components, *J. Chemometrics*, 2 (1988) 155–167
- [59] N.M. Faber, Critical evaluation of a significance test for partial least squares regression, *Anal. Chim. Acta*, 432 (2001) 235–240.
- [60] Q.S. Xu, Y.Z. Liang. Monte Carlo cross validation, *Chemom. Intell. Lab. Syst*, 56 (2001) 1–11.
- [61] R.L. Green, J.H. Kalivas, Graphical diagnostics for regression model determinations with consideration of the bias/variance trade-off, *Chemom. Intell. Lab. Syst*, 60 (2002) 173–188.
- [62] E.V. Thomas, Non-parametric statistical methods for multivariate calibration model selection and comparison, *J. Chemom*, 17 (2003) 653–659.
- [63] H. Seipel, J.H. Kalivas, Effective rank for multivariate calibration methods, *J. Chemom*, 18 (2004) 306–311.
- [64] Q.S. Xu, Y.Z. Liang, Y.P. Du, Monte Carlo cross-validation for selecting a model and estimating the prediction error in multivariate calibration, *J. Chemom*, 18 (2004) 112–120.
- [65] S. Wiklund, D. Nilsson, L. Eriksson, M. Sjöstrom, S. Wold, K. Faber, A randomization test for PLS component selection, *J. Chemom*, 21 (2007) 427–439.
- [66] N.M. Faber, R. Rajko, How to avoid over-fitting in multivariate calibration- the conventional validation approach and an alternative, *Anal. Chim. Acta*, 595 (2007) 98–106.
- [67] B. Efron, *The Jackknife, the Bootstrap, and Other Resampling Plans*. SIAM: Philadelphia, USA, 1982.
- [68] R. Wehrens, W.E. van der Linden, Bootstrapping principal component regression models, *J. Chemom*, 11 (1997) 157–171.

- [69] R. Wehrens, H. Putter, L.M.C. Buydens, The Bootstrap: A Tutorial, *Chemom. Intell. Lab. Syst.*, 54 (2000) 35–52.
- [70] S. Amato, V.E. Vinzi, Bootstrap-based Q2kh for the selection of components and variables in PLS regression, *Chemom. Intell. Lab. Syst.*, 68 (2003) 5–16.
- [71] T. Rebařka, S. Clemencon, M. Feinberg, Bootstrap-based tolerance intervals for application to method validation, *Chemom. Intell. Lab. Syst.*, 89 (2007) 69–81.
- [72] M.C. Denham, Choosing the number of factors in partial least squares regression: estimating and minimizing the mean squared error of prediction, *J. Chemom.*, 14 (2000) 351–361.
- [73] A. Hoskuldsson, Dimension of linear models, *Chemom. Intell. Lab. Syst.*, 32 (1996) 37–55.
- [74] M. Forina, S. Lanteri, Cerrato M.C. Oliveros, C. Pizarro Millan, Selection of useful predictors in multivariate calibration, *Anal. Bioanal. Chem.*, 380 (2004) 397–418.
- [75] B. Li, J. Morris, E.B. Martin. Model selection for partial least squares regression, *Chemom. Intell. Lab. Syst.* 64 (2002) 79–89.
- [76] L. Xu, Q.S. Xu, M. Yang, H.Z. Zhang, C.B. Cai, J.H. Jiang, H.L. Wu, R.Q. Yu, On estimating model complexity and prediction errors in multivariate calibration: generalized resampling by random sample weighting (RSW), *J. Chemometrics*, 25 (2011) 51–58
- [77] T. Næs, T. Isaksson, SEP or RMSEP, which is best?, *NIR news*, 2 (1991) 16
- [78] W. Wu, R. Manne, Fast regression methods in a Lanczos or PLS-1/ basis. Theory and applications, *Chemometrics and Intelligent Laboratory Systems*, 51 (2000) 145–161
- [79] K. Faber, B.R. Kowalski, Propagation of measurement errors for the validation of predictions obtained by principal components regression and partial least squares, *J. Chemometrics*, 11 (1997) 181–238.
- [80] J.H. Kalivas, J.B. Forrester, H.A. Seipel, QSAR modeling based on the bias/variance compromise: A harmonious and parsimonious approach, *Journal of Computer-Aided Molecular Design*, 18 (2004) 537–547.
- [81] H.A. Martens, P. Dardenne, Validation and verification of regression in small data sets, *Chemom. Intell. Lab. Syst.*, 44 (1998) 99–121.
- [82] J. Shao, Linear model selection by cross-validation, *J. Am. Statist. Assoc.*, 88 (1993) 486–494.
- [83] K. Baumann, Cross-validation as the objective function for variable-selection techniques. *Trends in Anal. Chem.*, 22 (2003) 395–406.
- [84] B.J. Kemps, W. Saeys, K. Mertens, P. Darius, J.G. De Baerdemaeker, B. De Ketelaere, The importance of choosing the right validation strategy in inverse modeling, *Journal, Near Infrared Spectrosc.*, 18 (2010) 231–237.
- [85] R. Marbach, T.H. Koschinsky, F.A. Gries, H.M. Heise, Non-invasive blood glucose assay by near infrared diffuse reflectance spectroscopy of the human Inner lip, *Appl. Spectrosc.*, 47 (1993) 875–881.
- [86] H.M. Heise, R. Marbach, Effect of data pretreatment on the non-invasive blood glucose measurement by diffuse reflectance NIR spectroscopy, *Proc Soc Photoinstrum Eng.*, 2089 (1994) 114–115.
- [87] M.A. Arnold, Small, G.W. Determination of physiological levels of glucose in an aqueous matrix with digitally filtered Fourier transform near-infrared spectra, *Anal Chem.*, 62 (1990) 1457–1464.
- [88] K.H. Hazen, M.A. Arnold, G.W. Small, Temperature-Insensitive Near-Infrared Spectroscopic Measurement of Glucose in Aqueous Solutions, *Applied Spectroscopy*, 48 (1994) 477–483.

- [89] H. Arimoto, M. Tarum, Y. Yamada, Temperature-Insensitive Measurement of Glucose Concentration Based on Near Infrared Spectroscopy and Partial Least Squares Analysis, *Optical Review*, 10 (2003) 74-76.
- [90] S. Sharma, M. Goodarzi, J. Delanghe, H. Ramon, W. Saeys, Using experimental data designs and multivariate modelling to assess the effect of glycated serum protein concentration on glucose prediction from near infrared spectra of human serum, *Applied Spectroscopy*, 68 (2014) 398-405
- [91] Y.C. Shen, A.G. Davies, E.H. Linfield, T.S. Elsey, P.F. Taday, D.D. Arnone. The Use of Fourier-Transform Infrared Spectroscopy for the Quantitative Determination of Glucose Concentration in Whole Blood. *Phys. Med. Biol.* 48 (2003) 2023-2032.
- [92] L.A. Marquardt, M.A. Arnold, G.W. Small, Near-Infrared Spectroscopic Measurement of Glucose in a Protein Matrix, *Anal. Chem.*, 65 (1993) 3271-3278
- [93] G.W. Small, M.A. Arnold, L.A. Marquardt, Strategies for Coupling Digital Filtering with Partial Least-Squares Regression: Application to the Determination of Glucose in Plasma by Fourier Transform Near-Infrared Spectroscopy, *Anal. Chem.*, 65 (1993) 3279-3289.
- [94] H. Ghung, M.A. Arnold, M. Rhiel, D.W. Murhammer, simultaneous measurement of glucose and glutamine in aqueous solutions by Near Infrared Spectroscopy, *Applied. Biochemistry and biotechnology*, 50 (1995) 109-125.
- [95] H. Chung, M.A. Arnold, M. Rhiel, D.W. Murhammer, Simultaneous Measurements of Glucose, Glutamine, Ammonia, Lactate, and Glutamate in Aqueous Solutions by Near-Infrared Spectroscopy, *Applied Spectroscopy*, 50 (1996) 270-276.
- [96] H.M. Heise, R. Marbach, T.H. Koschinsky, F.A. Gries, Noninvasive Blood Glucose Sensors Based on Near-Infrared Spectroscopy, *Artif. Organs*, 18 (1994) 439-447.
- [97] K.U. Jagemann, C. Fischbacher, K. Danzer, U.A. Muller, B.Z. Mertes, Application of Near-Infrared Spectroscopy for Non-Invasive Determination of Blood/Tissue Glucose Using Neural Networks, *Z Phys. Chem*, 191 (1995) 179-190.
- [98] M.A. Arnold, New Developments and Clinical Impact of Noninvasive Monitoring. In *Handbook of Clinical Laboratory Automation, Robotics, and Knowledge Optimization*; Kost, G. R., Ed.; John Wiley & Sons: New York, 1996; Chapter 12, pp 631-647.
- [99] S. Pan, H. Chung, M.A. Arnold, G.W. Small, Near-Infrared Spectroscopic Measurement of Physiological Glucose Levels in Variable Matrices of Protein and Triglycerides, *Anal Chem*, 68 (1996) 1124-1135.
- [100] K.H. Hazen, M.A. Arnold, G.W. Small, Measurement of glucose and other analytes in undiluted human serum with near-infrared transmission spectroscopy, *Analytica Chimica Acta*, 371 (1998) 255-267.
- [101] M. Ren, M.A. Arnold, Comparison of multivariate calibration models for glucose, urea, and lactate from near-infrared and Raman spectra, *Anal Bioanal Chem*, 387 (2007) 879-888.
- [102] J.S. Parab, R.S. Gad, G.M. Naik, Noninvasive glucometer model using partial least square regression technique for human blood matrix, *Journal of Applied Physics*, 107 (2010) 104701.
- [103] L. Xiaomei, W. Juan, Y. Qinghua, Wavelet analysis of near infrared spectral data in the application of Denoising, *Applied Mechanics and Materials*, 48 (2011) 1358-1362.
- [104] M.A. Arnold, J.J. Burmeister, G.W. Small, Phantom Glucose Calibration Models from Simulated Noninvasive Human Near-Infrared Spectra, *Anal. Chem.*, 70 (1998) 1773-1781.
- [105] P. Comon, Independent Component Analysis, a new concept?, *Signal Processing*, 36 (1994) 287-314.

- [106] D.N. Rutledge, D. Jouan-Rimbaud Bouveresse, Independent Components Analysis with the JADE algorithm, *Trends in Analytical chemistry*, 50 (2013) 22–32
- [107] A. Al-Mbaideen, M. Benaissa, Determination of glucose concentration from NIR spectra using independent component regression, *Chemometrics and Intelligent Laboratory Systems*, 105 (2011) 131–135.
- [108] S. Sharma, M. Goodarzi, L. Wynants, H. Ramon, W. Saeys, Efficient use of pure component and interferent spectra in multivariate calibration, *Analytica Chimica Acta*, 778 (2013) 15– 23
- [109] D.M. Haaland, L. Han, T.M. Niemczyk, Use of CLS to Understand PLS IR Calibration for Trace Detection of Organic Molecules in Water, *Applied Spectroscopy*, 53 (1999) 390-395.
- [110] D.M. Haaland, D.K. Melgaard, New Augmented classical least squares methods for improved quantitative spectral analysis, *Vibrational Spectroscopy*, 29 (2002) 171-175.
- [111] D.K. Melgaard, D.M. Haaland, C.M. Wehlburg, Concentration Residual Augmented Classical Least Squares (CRACLS): A Multivariate Calibration Method with Advantages over Partial Least Squares, *Applied Spectroscopy*, 56 (2002) 615–624.
- [112] D.M. Haaland, D.K. Melgaard, New Prediction-Augmented Classical Least-Squares (PACLS) Methods: Application to Unmodeled Interferents, *Applied Spectroscopy*, 54 (2000) 1303-1312
- [113] W. Saeys, K. Beullens, J. Lammertyn, H. Ramon, T. Naes, Increasing Robustness against Changes in the Interferent Structure by Incorporating Prior Information in the Augmented Classical Least-Squares Framework, *Anal. Chem.* 80 (2008) 4951–4959
- [114] D.M. Haaland, D.K. Melgaard, New classical least-squares/partial least-squares hybrid algorithm for spectral analyses, *Appl. Spectrosc.* 55 (2001) 1–8.
- [115] J. Claude Boulet, J.M. Roger, Improvement of Direct Calibration in spectroscopy, *Analytica Chimica Acta*, 668 (2010) 130-136.
- [116] R. Marbach, On Wiener filtering and the physics behind statistical modeling, *J. Biomed. Opt.* 7 (2002) 130-147
- [117] R. Marbach, A New Method for Multivariate Calibration, *J. Near Infrared Spectroscopy*, 13 (2005) 241– 254
- [118] R. Neruda, P. Vidnerov, Learning Errors by Radial Basis Function Neural Networks and Regularization Networks, *International Journal of Grid and Distributed Computing*, 1 (2009) 49-58
- [119] M. Goodarzi, M.P. Freitas, Y. Vander Heyden, Linear and nonlinear quantitative structure–activity relationship modeling of the HIV-1 reverse transcriptase inhibiting activities of thiocarbamates, *Analytica Chimica Acta*, 705 (2011) 166-173
- [162] E.P.P.A. Derks, M.S. Sanchez Pastor, L.M.C. Buydens, Robustness analysis of radial base function and multi-layered feed-forward neural network models, *Chemom. Intell. Lab. Syst.* 28 (1995) 49–60.
- [121] C. Fischbacher, K.U. Jagemann, K. Danzer, U.A. Müller, L. Papenkordt, J. Schüler, Enhancing calibration models for non-invasive near-infrared spectroscopical blood glucose determination, *Fresenius J Anal Chem*, 359 (1997) 78–82.
- [122] M. Goodarzi, B. Dejaegher, Y. Vander Heyden, Feature Selection Methods in QSAR Studies, *J AOAC Int.* 95 (2012) 636-651.
- [123] D.M. Haaland, M.R. Robinson, G.W. Koepp, E.V. Thomas, R.P. Eaton, Reagentless Near-Infrared Determination of Glucose in Whole Blood Using Multivariate Calibration, *Applied Spectroscopy*, 46 (1992) 1575-1578.

- [124] S. Kasemsumran, Y.P. Du, K. Maruo, Y. Ozaki, Improvement of partial least squares models for in vitro and in vivo glucose quantifications by using near-infrared spectroscopy and searching combination moving window partial least squares, *Chemometrics and Intelligent Laboratory Systems*, 82 (2006) 97-103.
- [125] A. Niazi, R. Leardi, Genetic algorithms in chemometrics, *J. Chemometrics*, 26 (2012) 345-351
- [126] R.E. Shaffer, G.W. Small, M.A. Arnold, Genetic Algorithm-Based Protocol for Coupling Digital Filtering and Partial Least-Squares Regression: Application to the Near-Infrared Analysis of Glucose in Biological Matrices, *Anal. Chem.*, 68 (1996) 2663-2675
- [127] A.S. Bangalore, R.E. Shaffer, G.W. Small, M.A. Arnold, Genetic Algorithm-Based Method for Selecting Wavelengths and Model Size for Use with Partial Least-Squares Regression: Application to Near-Infrared Spectroscopy, *Anal. Chem.*, 68 (1996) 4200-4212
- [128] Q. Ding, G.W. Small, M.A. Arnold, Genetic Algorithm-Based Wavelength Selection for the Near-Infrared Determination of Glucose in Biological Matrixes: Initialization Strategies and Effects of Spectral Resolution, *Anal. Chem.*, 70 (1998) 4472-4479.
- [129] J. Chen, M.A. Arnold, G.W. Small, Comparison of Combination and First Overtone Spectral Regions for Near-Infrared Calibration Models for Glucose and Other Biomolecules in Aqueous Solutions, *Anal. Chem.*, 76 (2004) 5405-5413.
- [130] H.M. Heise, R. Marbach, A. Bittner, T. Koschinsky, Clinical chemistry and near infrared spectroscopy: multicomponent assay for human plasma and its evaluation for the determination of blood substrates, *J. Near Infrared Spectrosc.*, 6 (1998) 361-374.
- [131] S. Kasemsumran, Y. Du, K. Murayama, M. Huehne, Y. Ozaki, Simultaneous determination of human serum albumin, γ -globulin, and glucose in a phosphate buffer solution by near-infrared spectroscopy with moving window partial least-squares regression, *Analyst*, 128 (2003) 1471-1477.
- [132] A.K. Amerov, J. Chen, G.W. Small, M.A. Arnold, Scattering and Absorption Effects in the Determination of Glucose in Whole Blood by Near-Infrared Spectroscopy, *Anal. Chem.*, 77 (2005) 4587-4594.
- [133] K.H. Hazen, M.A. Arnold, G.W. Small, Measurement of Glucose in Water with First-Overtone Near-Infrared Spectra, *Applied Spectroscopy*, 52 (1998) 1597-1605
- [134] A. Rinnan, F. Berg, S.B. Engelsen, Review of the most common pre-processing techniques for near-infrared spectra, *TrAC Trends in Analytical Chemistry*, 28 (2009) 1201-1222
- [135] J. Engel, J. Gerretzen, E. Szymanska, J.J. Jansen, G. Downey, L. Blanchet, L.M.C. Buydens, Breaking with trends in pre-processing?, *Trends in Analytical chemistry*, 50 (2013) 96-106.
- [136] K.M. Pierce, B. Kehimkar, L.C. Marney, J.C. Hoggard, R.E. Synovec, Review of chemometric analysis techniques for comprehensive two dimensional separations data, *Journal of Chromatography A*, 1255 (2012) 3-11
- [138] S. Sharma, M. Goodarzi, H. Ramon, W. Saeys, Using Performance evaluation of preprocessing techniques utilizing expert information in multivariate calibration, *Talanta*, 121 (2014) 105-112 .
- [139] S. Pieters, W. Saeys, T. Van den Kerkhof, M. Goodarzi, M. Hellings, T. De Beer, Y. Vander Heyden, Robust calibrations on reduced sample sets for API content prediction in tablets: Definition of a cost-effective NIR model development strategy, *Analytica Chimica Acta*, 761(2013) 62-70.

[140] J.A. Fernandez Pierna, F. Chauchard, S. Preys, J.M. Roger, O. Galtier, V. Baeten, P. Dardenne, How to build a robust model against perturbation factors with only a few reference values: A chemometric challenge at ‘Chimiométrie 2007’, *Chemom Intell Lab Syst*, 106 (2011) 152–159.

[141] Y.P. Du, Y.Z. Liang, S. Kasemsumran, K. Maruo, Y. Ozaki, Removal of interference signals due to water from in vivo near-infrared (NIR) spectra of blood glucose by region orthogonal signal correction (ROSC), *Anal Sci*. 20 (2004) 1339-1345.

Captions

Fig. 1. Overview of different strategies for blood-glucose monitoring.

Fig. 2. Molar absorptivity spectra of water and glucose in the first overtone (a and b) and combination band (c and d) regions, respectively.

Fig. 3. Bias and variance trade-off to prediction error as a function of model complexity (number of Principal Components or Latent Variables) [84,95].

Table 1.
Summary overview of case studies discussed in the text

Method	Matrix	Glucose range	Wavelengths	Ref.
Univariate Calibration	0.1 M phosphate buffer at pH 7.2	1-20 mM	2273 nm	[87]
PLS and using Fourier Filtering as preprocessing	Bovine serum albumin + 0.1 M phosphate buffer (pH 7.2)	1-20 mM	2000-2500 nm	[92]
	Plasma	2.5-25.5 mM		[93]
	Phosphate buffer at 37°C. Test set spectra collected at temperatures ranging from 32 to 41°C with 1°C increments.	1.25-19.66 mM		[88]
	Aqueous solution of a binary mixture of glucose and glutamine	1.66-59.91 mM		[94]
	1- Phosphate buffer with five unique levels of triacetin. 2- Phosphate buffer with 10 different Bovine Serum Albumin (BSA) concentrations.	1- 2-20 mM 2- 1.25- 20 mM		[99]
	Aqueous solution of Glutamine, Ammonia, Lactate and Glutamate	5.5-100 mM		[95]
PLS	Human serum	3.1-31.8 mM		[100]

GA	1- Triacetone and bovine serum albumin (160 samples) 2- Human serum (238 samples) 3- Bovine blood (35 samples)	For three data sets 1-20 mM		[126]
GA and Grid Search	1- Methyl isobutyl ketone in water (17 samples) 2- Phosphate buffer with bovine serum albumin and triacetin [taken from 126] 3- Human serum [taken from 126]	1-20 mM		[127]
GA	Data sets from ref [126]	1-20 mM		[128]
PLS and Grid Search for variable selection NAS	Phosphate buffer solution with lactate and urea.	1-30 mM	For NIR 2000- 2500 nm For Raman 2898-100000 nm	[101]
PLS and NAS	Whole bovine Blood	3-30 mM	1111-1851 nm 2000-2500 nm	[132]
	Buffer solution with Lactate, Urea, ascorbate triacetin and alanine	1-35 mM	1538-1818 nm 2000-2500 nm	[129]
PLS	Spectra measured through different people with diabetes	-	900-1200 nm	[97]
PLS	Aqueous solutions at different temperatures varying from 25 to 35 °C	55-166 mM	1250-1800 nm	[89]
PLS ICA and PCA	Phosphate buffer with urea and triacetin	2.7-25 mM	2100-2400 nm	[107]
SCMWPLS	1- Bovine serum	1- 1.6-83.19 mM	For the first data set 1280-1849 nm	[124]
	2- Forearm of a healthy man	2- 2.2-10 mM	For the second data set 1212-1889 nm	
MWPLS	Buffer matrix with albumin and globulin protein	-	833-2500 nm	[130]
	Plasma with protein, cholesterol and triglycerides	0-111 mM	1470-2381 nm	[131]
PLS, NAP/CLS, ACLS, IDC and SBC	1- Aqueous solutions with Na-d-lactate and urea	1- 1-30 mM	First data set 1525 to 1825 nm	[108]
	2- Powders of casein and lactate	2- 0-86.9 %	Second data set 1100-2500 nm	
EMSC, SIS, EPO, GLSW,	1- Aqueous solutions with Na-d-lactate and urea	1- 1-30 mM	First data set 1525 to 1825	[137]
		2- 0-86.9 %		

	2- Powders of casein and lactate [113]		nm Second data set 1100-2500 nm	
PLS and RBFNN	Spectra measured through Fingers of diabetic type 1 people	4-16 mM	850-1350 nm	[121]
OSC, ROSC , PLS	Spectra measured through skin	4.43-9.77 mM	1212-1889 nm	[140]

Accepted Manuscript